

Growth and division mode plasticity by cell density in marine-derived black yeasts

Gohta Goshima^{1,2}

¹ Sugashima Marine Biological Laboratory, Graduate School of Science, Nagoya University, Sugashima, 429-63, Toba 517-0004, Japan

² Division of Biological Science, Graduate School of Science, Nagoya University, Furocho, Chikusa-ku, Nagoya 464-8602, Japan

Email: goshima@bio.nagoya-u.ac.jp; Phone: +81 599-34-2216

Abstract

The diversity and ecological contribution of the fungus kingdom in the marine environment remain under-studied. A recent survey in the Atlantic (Woods Hole, MA, USA) brought to light the diversity and unique biological features of marine fungi. The study revealed that black yeast species undergo an unconventional cell division cycle, which has not been documented in conventional model yeast species such as *Saccharomyces cerevisiae* (budding yeast) and *Schizosaccharomyces pombe* (fission yeast). The prevalence of this unusual property is unknown. Inspired by the findings in Woods Hole, I collected and identified >50 marine fungi species across 40 genera from the ocean surface, sediment, and macroalgal surface in the Pacific (Sugashima, Toba, Japan). The Sugashima collection largely did not overlap with the Woods Hole collection and included several unidentifiable species, further illustrating the diversity of marine fungi. Three black yeast species were isolated, two of which were commonly found in Woods Hole (*Aureobasidium pullulans*, *Hortaea werneckii*). Surprisingly, I observed that their cell division mode was dependent on cell density, and the previously reported unconventional division mode was reproduced only at a certain cell density. For all three black yeast species, cells underwent filamentous growth with septations at low cell density and immediately formed buds at high cell density. At intermediate cell density, two black yeasts showed rod cells undergoing septation at the cell equator, in a manner similar to *S. pombe*. In contrast, all eight budding yeast species showed a consistent division pattern regardless of cell density. In five budding yeast species, the mother cell formed a single bud at a time at an apparently random site, similar to *S. cerevisiae*. The other three budding yeast species possessed a fixed budding site. This study illustrates the plastic nature of the growth/division mode of marine-derived black yeast.

Introduction

Understanding the habitats of marine organisms is important for understanding marine ecology. Much of this effort has been put on macro-organisms, such as fishes, benthic organisms, and invertebrates, as well as unicellular microorganisms such as algae and bacteria [1]. Relatively little attention has been paid to fungi, and little is known about their life cycle and physiology [2, 3]. The genetics and cell biology of these organisms have been pioneered in a few terrestrial fungal systems, such as *Saccharomyces cerevisiae*, *Schizosaccharomyces pombe*, and *Aspergillus nidulans* [4-6]. An important step towards understanding the ecology of marine fungi is the identification of fungi in various locations.

47 An interesting study was published in 2019, in which 35 fungi were collected from
48 the sediment, surface ocean water, and benthic animals (corals, sponges) around Woods
49 Hole, MA, USA. That study investigated the division pattern of several black yeast
50 species via live imaging and found remarkable unconventional features in their cell
51 division cycle [7]. For example, a single *Hortaea werneckii* cell always underwent fission
52 during its first cell division, but the next division involved budding at 92% probability.
53 This observation challenged the conventional view that a single cell division pattern is
54 intrinsic to a yeast species; for example, *S. pombe* and *S. cerevisiae* always divide via
55 fission or budding, respectively. In another striking example, more than 50% of
56 *Aureobasidium pullulans* cells produced multiple rounds of simultaneous buds, which is
57 never observed in *S. cerevisiae* [7]. From an ecological point of view, this study urges the
58 necessity of further sampling and characterisation, as what has been reported to date is
59 unlikely to be the full set of marine fungi in the ocean.

60 Inspired by [7], I collected free-living marine fungi in front of Nagoya University's
61 Marine Biological Laboratory (NU-MBL) on Sugashima Island, Toba, Japan (Fig. 1A).
62 The species were identified via DNA barcode sequencing, and the division pattern was
63 observed for budding and black yeasts (no fission yeast was isolated). The collected
64 species, or even genera, were only partially overlapped with [7], suggesting the existence
65 of highly divergent fungal species in the ocean. Surprisingly, the division pattern of black
66 yeasts (*H. werneckii*, *A. pullulans*, and other unidentified species) was initially
67 inconsistent with those previously reported in [7], and this enigma was solved through
68 the observation of cell density-dependent alterations in their division patterns.

69

70 **Materials and methods**

71

72 *Isolation of marine fungi at NU-MBL*

73 Samples were collected for 8 days from 4th March to 5th June 2020, in which the majority
74 were obtained on the 22nd and 23rd of April. The ocean water temperature was 15.5 °C
75 and the salinity was 34.9 ‰. This salinity indicates that there was no significant fresh
76 water flow into this area from the large rivers in Ise Bay. Surface water samples were
77 collected at the pier of the NU-MBL using a plastic bucket (Lat. 34°29'8"N, Long.
78 136°52'32"E) (Fig. 1B, green). One litre of seawater was filtered using a 0.45-µm
79 Millipore Stericup to obtain a 100× concentration. One millilitre of the concentrate was
80 spread onto three types of media, which were similar to those used in [7]: YPD (10 g/L
81 yeast extract, 10 g/L peptone [Bacto tryptone], 20 g/L glucose, 12 g/L agar), malt medium
82 (20 g/L malt extract, 6 g/L tryptone, 20 g/L glucose, 12 g/L agar), and potato dextrose
83 (24 g/L potato dextrose broth, 12 g/L agar). All species tested could grow on any medium;
84 retrospectively, the preparation of three different media was not needed. Sediment
85 samples were collected once by taking the mud at the bottom of the outside tank (Fig.
86 1C). Seaweeds were collected from the intertidal zone in front of the NU-MBL (Fig. 1B,
87 magenta). Approximately 3 cm × 3 cm fragments of seaweed were obtained, which were
88 rinsed with semi-sterile seawater (~500 mL) three times, followed by knife-cutting into
89 small pieces and spreading onto a plate (Fig. 1D). All media were made with seawater at
90 NU-MBL, which was pre-filtered with ADVANTEC filter paper #2. Antibiotics were
91 added to the medium to avoid bacterial growth (20 µg/mL carbenicillin, 100 µg/mL
92 chloramphenicol, 10 µg/mL tetracycline) [7]. All fungal isolates were stored at -80 °C in
93 YPD medium containing 20% glycerol.

94

95 *PCR and sequencing*

96 The ITS and NL sequences were sequenced for all strains using the primers listed in Table
97 1 [7]. If the species could not be determined through these two sequences, the β -tubulin
98 gene locus was amplified and sequenced. PCR was performed with the KOD-ONE kit
99 (TOYOBO) using a colony or the extracted genomic DNA as the template. DNA
100 extraction was performed by boiling a piece of fungal colony for 5 min in 0.25% SDS
101 followed by table-top centrifugation.

102

103 **Table 1: Primers used in this study**

Locus	Primer ID	Primer sequences
ITS1/4	7577-ITS1 (fungi)	TCCGTAGGTGAACCTGCGG
	7578-ITS4 (fungi)	TCCTCCGCTTATTGATATGC
NL1/4	7579-NL1 (fungi)	GCATATCAATAAGCGGAGGAAAAG
	7580-NL4 (fungi)	GGTCCGTGTTTCAAGACGG
β -Tubulin	7607-fungal-b-tub-Fw1	CGTGACAGGGTAACCAAATTGGTG
	7608-fungal-b-tub-Fw2	GAGCCCGGTACCATGGACG
	7609-fungal-b-tub-Rv1	GGTGATCTGGAAACCCTGGAGG
	7610-fungal-b-tub-Rv2	CCCATACCGGCACCGGTACC

104

105 *Species identification*

106 Sequence homology was determined using the BLASTN program. If both ITS and NL
107 sequences were perfectly matched to a single species, the fungal isolate was concluded to
108 be the species. If not, the β -tubulin sequences were also used. In some cases, either the
109 ITS or NL sequences had a 100% match to a certain species, whereas the other did not
110 show an exact match. When the mismatch was less than 3 bp, the fungal isolate was likely
111 the species with a slight strain-specific sequence variation, whereas a >3 bp mismatch in
112 two or three barcodes led to the assignment of possible novel species or genera. All the
113 barcode sequences are presented in Table S1.

114

115 *Live microscopy*

116 Initially, cells grown on the YPD plate were directly inoculated into YPD liquid medium
117 in an 8-well glass-bottom dish (Iwaki). However, the division modes were not consistent
118 between experiments for some species. Therefore, cells were grown in a YPD liquid
119 medium until saturation and inoculated into an 8-well plate after cell counting (300 μ L
120 culture volume). Note that this liquid-based imaging condition is different from that in
121 [7], in which agar pads were used. The growths of 10^3 , 10^4 , 10^5 , and $>10^5$ cells were
122 compared for black yeasts. Transmission light imaging was carried out at 23 °C with a
123 Nikon inverted microscope (Ti) with a 40 \times 0.95 NA lens (Plan Apo) and a Zyla CMOS
124 camera (Andor). The brightness and contrast of the obtained images were adjusted using
125 FIJI software. For DNA imaging of *Hortaea werneckii*, cells were cultured with a more
126 transparent medium. Synthetic minimal medium, similar to what was used for *Aspergillus*
127 *nidulans*, was made with sea water (6 g/L NaNO₃, 0.52 g/L KCl, 1.52 g/L KH₂PO₄, 10
128 g/L glucose, 1.5 mL trace elements, 10 mg/L biotin, 0.25 g/L MgSO₄, pH = 6.5 [adjusted
129 with NaOH]) [8]. Hoechst 33342 was added at 3–6 μ g/mL (final). DNA imaging was
130 performed with another Nikon inverted microscope (Ti2) attached to a 100 \times 1.40 NA lens,

131 a 405-nm laser, CSU-10 spinning-disc confocal unit, and the CMOS camera Zyla (at
132 23 °C). The time intervals used were mostly 2 min, but sometimes 2.5 min or 5 min was
133 used. The microscopes were controlled using NIS Elements software (Nikon).

134

135 **Results and Discussion**

136

137 **Isolation of fungi at the Sugashima marine laboratory**

138 Fungi were isolated from three sources: surface ocean sea water near the beach (Fig. 1B,
139 green), an outdoor tank that has various benthic animals and seaweeds (circulated surface
140 water and sediment; Fig. 1C), and sliced seaweeds (each ~3 cm) that were collected in
141 the intertidal zone in front of the laboratory (Fig. 1B [magenta], D). The sediment was
142 most enriched with fungi (Fig. 1E; 200 µL sediment). Fungal colonies were obtained from
143 100 mL surface sea water, and 7.5 ± 8.5 fungal colonies were obtained ($n = 6$), whereas
144 seaweeds were a more abundant source of fungi (25 ± 26 colonies isolated from a ~3 cm
145 piece of seaweed body [$n = 10$]). However, based on colony colour, it was deduced that
146 many colonies were derived from the same species. In total, 74 colonies were regrown on
147 separate plates (four examples are shown in Fig. 1F), and two or three barcode regions
148 were sequenced. For some clones, the species or even genera could not be identified
149 because of the high deviation of the barcode sequences from the known sequences
150 registered in the database (named with “sp” or described as “unclear” in Table 2). The
151 total number of species identified was 50–65, depending on whether several clones (e.g.
152 *Cladosporium*) were considered to be the same species (Table 2).

153

154 **Comparison with the Woods Hole collection**

155 There were considerable differences between the current collection at Sugashima and
156 what was identified around Woods Hole [7] (Table 2, right column). Only six species
157 were isolated in both studies (*Aureobasidium pullulans*, *Cladosporium halotolerans*,
158 *Hortaea werneckii*, *Metschnikowia bicuspidate*, *Meyerozyma guilliermondii*, and
159 *Parengyodontium album*). At the genus level, only seven genera were common
160 (*Aspergillus*, *Candida*, *Epicoccum*, *Filobasidium*, *Penicillium*, *Rhodotorula*, and
161 *Trichoderma*), while other genera were uniquely isolated in either location: 27 from
162 Sugashima (*Alternaria*, *Arthopyrenia*, *Arthrimum*, *Cystobasidium*, *Diaporthe*, *Didymella*,
163 *Fusarium*, *Kluyveromyces*, *Letendraea*, *Leucosporidium*, *Microdochium*, *Neoascochyta*,
164 *Neopestalotiopsis*, *Paraboeremia*, *Paradendryphiella*, *Pestalotiopsis*, *Phacidium*, *Phoma*,
165 *Pyrenochaetopsis*, *Simplicillium*, *Sphaerulina*, *Umbelopsis*, *Ustilago*, and four unclear
166 genera), and six from Woods Hole (*Apiotrichum*, *Cadophora*, *Cryptococcus*, *Exophiala*,
167 *Knufia*, *Phaeotheca*). While this discrepancy may partly stem from seasonal or regional
168 differences, it more likely reflects the limited coverage of fungi in both studies. My survey
169 agrees with the current view that many more species exist in the ocean [3].

170

171 **Budding yeast species with fixed and variable bud positions**

172 Fifteen fungal species produced yeast-like colonies on culture plates (Fig. 1F, second
173 image). Live imaging was performed for these species at least thrice at different cell
174 densities. Five of them turned out to have *S. cerevisiae*-like budding-growth cycles, where
175 a daughter cell emerged from the round-shaped mother cell and a mother cell can produce
176 a second daughter at other sites than the previous one (*Candida sake*, *Kluyveromyces*
177 *nonfermentans*, *Metschnikowia bicuspidate*, *Meyerozyma guilliermondii*, *Rhodotorula*

178 *sp.*) (Fig. 2A, Video 1). Interestingly, the budding sites of three other yeasts were fixed,
179 although the mother cell had a nearly round shape (*Cystobasidium slooffiae*, *Filobasidium*
180 *magnum*, *Filobasidium sp.*) (Fig. 2B, Video 1). Four other fungi were rod-shaped, in
181 which fission and/or budding were observed (*Leucosporidium intermedium*, *Ustilago sp.*,
182 *Sphaerulina rhabdoclinis*, *Sphaerulina sp.*) (Video 2).

183

184 **Cell density-dependent division pattern alteration in the black yeast *A. pullulans***

185 The remaining three fungi that formed yeast-like colonies produced black or brown
186 pigment. Two of them have been extensively studied by [7]: *A. pullulans* (Fig. 3A) and
187 *H. werneckii* (Fig. 4A). *A. pullulans* in [7] had a round shape and showed multiple buds
188 at one site. However, in my first few imaging attempts, such a characteristic division
189 pattern was never observed. Instead, they first grew as filaments, and later produced
190 multiple buds from many locations on the filament. In the course of repetitive imaging, it
191 was noticed that a division pattern closer to that described in [7] could be obtained when
192 the initial cell density was increased. To test the possibility that the division pattern is
193 density-dependent, a 10-fold dilution series of the strain was prepared for imaging
194 (relative cell densities: $\times 1$, $\times 10$, $\times 100$, and $\times 1000$). When the initial cell density was low,
195 a single cell first elongated with occasional septation, followed by multiple budding from
196 the elongated cell filament (100%, $n = 50$) (Fig. 3B, D, Video 3). The higher the cell
197 density, the faster the bud emerged (Fig. 3C). Immediate budding without extensive
198 mother cell elongation or septation was observed only when the initial cell density was
199 high (Fig. 3B, 19 out of 30 cells). However, the majority of the cells (14/19) showed buds
200 at both poles of the mother cell (Fig. 3E) rather than produced buds from the same pole,
201 as reported in [7] (5/19) (Fig. 3F). Thus, this black yeast species showed division pattern
202 variation depending on the cell density.

203 It should be noted that the identity of the bud is unknown. An earlier study involving
204 immunofluorescence microscopy of microtubules and actin interpreted that the buds were
205 conidia (asexual spores) [9]. This is a possible interpretation.

206

207 **Cell density-dependent division pattern alteration in the black yeast *H. werneckii***

208 Two clones of *H. werneckii* were isolated, and their colony growth rates were slightly
209 different (Fig. 4A). The barcode sequences had high similarity but were not identical (1
210 bp mismatch). These were interpreted as natural variants of the same species. Imaging of
211 these clones initially produced puzzling results: the reported characteristic division
212 pattern— a single cell almost always undergoes fission, followed by budding [7] – was
213 rarely observed. To test the possibility that, similar to *A. basidium*, the initial cell density
214 might have affected the division pattern, the number of inoculated cells was varied ($\times 1$,
215 $\times 10$, $\times 100$, $\times 300$). The initial cell numbers dramatically affected the mode of the first few
216 cell divisions in both isolates (Fig. 4B presents the result of NU28; Video 4). Multiple
217 rounds of septation were observed when cell density was low and multiple budding
218 occurred hours later (Fig. 4B, D). The higher the cell density, the earlier the bud emerged
219 (Fig. 4C). In contrast, the reported mode of division – fission followed by budding – was
220 predominantly observed when the cell density was high (Fig. 4B, E). However, cells that
221 formed buds without fission were also observed, which was not reported in [7] (Fig. 4B,
222 F). Thus, the division pattern variability of our *H. werneckii* strain was similar to that of
223 *A. pullulans*.

224

225 **Cell density-dependent division pattern alteration in an unidentified black yeast**
226 **species**

227 In the present study, another yeast strain (NU30) formed dark brown-coloured colonies
228 on the plate (Fig. 5A). The barcode sequences did not perfectly match any registered
229 species; because the mismatch was large, the name of this yeast could not be determined.
230 To reveal its growth/division pattern and test if it was altered depending on the initial cell
231 density, time-lapse imaging was conducted at four different initial cell densities ($\times 1$, $\times 10$,
232 $\times 100$, and $\times 700$). The cell division pattern observed was remarkably similar to that of *H.*
233 *werneckii* (Fig. 5B–F, Video 5). Budding occurred after multiple septations when the
234 initial cell density was low, whereas a mother cell, without cell septation, produced
235 multiple buds sequentially from the same site (blue and magenta arrows) when the initial
236 cell density was high (Fig. 5E, F).

237
238 **Nuclear segregation scales with cell length in *H. werneckii***

239 In the model budding yeast *S. cerevisiae*, budding starts at the G1/S transition of the cell
240 cycle, and nuclear division takes place when the bud reaches a certain size [10]. In *S.*
241 *pombe*, the nucleus is kept in the centre of the cell during interphase (mostly G2 phase),
242 then mitotic commitment occurs when the cell reaches a certain length ($\sim 14 \mu\text{m}$) [11]. In
243 both cases, cell division (septation) occurs immediately after nuclear division, producing
244 daughter cells that have an identical shape to the mother. In contrast, in *A. nidulans* and
245 *Ashbya gossypii*, the model filamentous fungi, multiple nuclear divisions take place
246 without septation in the tip-growing cells, resulting in the production of multinucleated
247 cells [12, 13]. I was curious whether nuclear and cell divisions were coupled in the above
248 three black yeast species, whose division pattern was flexible.

249 To follow nuclear division and septation/budding in live cells, their nuclei were
250 stained with Hoechst 33342, which is known to be permeable in many cell types,
251 including *S. pombe* [14]. However, staining and live imaging of *A. pullulans* and NU30
252 were not successful. In contrast, *H. werneckii* was stainable, and its nuclear dynamics was
253 observable in real time (Fig. 6, Video 6, 7). Therefore, time-lapse imaging with Hoechst
254 33342 using a spinning-disc confocal microscope was performed for *H. werneckii*.

255 In the budding type of mitosis shown in Fig. 6A, which prevailed when the cell
256 density was high, nuclear separation occurred when the bud size reached $60 \pm 11 \%$ (\pm
257 SD) of the mother ($n = 30$). The nucleus was positioned in the mother, slightly on the bud
258 neck side at the time of chromosome condensation (i.e. mitotic entry) ($44 \pm 6 \%$ position
259 from the bud neck). Sister chromatid separation occurred in the mother, and one of the
260 sister chromatids moved into the bud. Kymograph analysis indicated that the sister
261 chromatid motility relative to the cell edge was asymmetric (Fig. 6A, bottom): the sister
262 on the bud side moved much longer distances, whereas the sister in the mother moved
263 much less or sometimes showed bud-oriented movement. The maximum distance
264 between sister chromatids was $9.4 \pm 1.1 \mu\text{m}$, which was comparable to the mother cell
265 length ($9.2 \pm 1.0 \mu\text{m}$) and was 36 % shorter than the entire cell length (i.e., daughter +
266 mother length). These results suggested that the anaphase spindle was motile in the cell.
267 The mitotic duration (chromosome condensation to anaphase onset) was 14 ± 7 min.
268 Septation, which was indicated by a straight line of the Hoechst dye at the bud neck, was
269 completed 16 ± 6 min after sister chromatid separation.

270 In the fission type of mitosis shown in Fig. 6B, the nucleus was positioned near the
271 centre of the cell at the time of chromosome condensation ($50 \pm 5 \%$ position along the

272 cell axis, $n = 20$). After 16 ± 3 min, the sister chromatids were separated. Unlike in *S.*
273 *pombe*, chromosome segregation did not always occur symmetrically (232–236 min time
274 point in Video 6) and the chromatids rarely reached the cell edge (maximum sister
275 chromatid distance was 5.6 ± 0.5 μm , which was 54 ± 5 % of cell length) (Fig. 6B, bottom).
276 Septation was completed in the middle of the cell at 29 ± 4 min after sister chromatid
277 separation.

278 In the tip-growing cells, which were observed at low cell density, a single nucleus
279 was detected, and it moved apically during tip growth, contrary to the multiple nuclei in
280 *A. nidulans* or *A. gossypii* (Fig. 6C and 6D; flare-like structures were also stained by
281 Hoechst 33342). Therefore, the nucleus stayed near the centre of the cell (46 ± 5 %
282 position from the tip at mitotic entry, $n = 15$). The cell length was quite variable at the
283 time of chromosome condensation (34 ± 10 μm , $\pm\text{SD}$, $n = 15$); in some cases, it reached
284 >40 μm , which was four times longer than the rod-shaped or budding cells described
285 above. Mitotic duration was shorter than that in other types (9 ± 1 min, $n = 9$). Sister
286 chromatids moved longer distances (52 ± 7 % of the cell length, $n = 14$) and septation
287 occurred in the middle of the two nuclei at 22 ± 4.5 min ($n = 8$) after sister chromatid
288 separation. However, the middle part was motile during anaphase, implying that the
289 anaphase spindle was motile in the cell. Consequently, the chromosome position at
290 metaphase was not always consistent with the septation position (Fig. 6D).

291 Thus, despite variations in cell size and geometry (rod, filament, bud), septation was
292 coupled with nuclear division. However, the segregating distance of sister chromatids
293 varied significantly, scaling with the cell length and shape.

294

295 **Conclusions**

296 Two major conclusions can be drawn from this study. First, a very limited local survey
297 has increased the list of marine-derived fungi, illustrating their diversity in the ocean. The
298 species could not be determined for several fungi, suggesting that they might represent
299 undescribed species. More comprehensive sampling and taxonomic analyses are needed
300 to further expand the list of fungi from the ocean. Second, the collected black yeast
301 species changed their division mode depending on the cell density. This plasticity may be
302 beneficial for them, particularly when they reside on the surfaces of animals and
303 macroalgae. Filamentous growth with branching is an excellent means to explore
304 unoccupied areas, whereas budding in a crowded environment allows the clone to be
305 released to the free water and translocated to other animal/algae surfaces. This property
306 somewhat resembles that of filamentous fungi such as *Aspergillus*; they exhibited 2D
307 hyphal growth, followed by conidia (asexual spores) release [15]. Switching between
308 yeast-like budding and hyphal growth has also been reported for the pathogenic fungus
309 *Candida albicans* [16, 17]. However, the filament was curved and area exploration was
310 not optimised for *H. werneckii* and NU30; hence, the advantage of this growth/division
311 mode remains unclear. Combined with this and previous studies [7], all five observed
312 black yeast species showed at least two growth/division patterns. Elucidating the
313 chemical and/or physical cues that trigger the division mode alteration and the prevalence
314 of plasticity in marine fungi would be interesting topics for future research.

315

316 **Acknowledgements**

317 I am grateful to Tomoya Edzuka and Maki Shirae-Kurabayashi for seaweed collection,
318 Masahiro Suzuki (Kobe University) for help with seaweed identification, Masashi

319 Fukuoka for daily temperature and salinity measurements, Naoto Jimi for helpful
320 comments on taxonomy, and Amy Gladfelter (Marine Biological Laboratory, Woods
321 Hole/University of North Carolina) for the introduction to marine fungal biology and
322 encouraging sample collection on the Japanese coast. This work was supported by JSPS
323 KAKENHI (17H06471, 18KK0202).

324

325 References

326

- 327 1. OBIS (ocean biodiversity information system). <https://obis.org/>.
- 328 2. Gladfelter, A.S., James, T.Y., and Amend, A.S. (2019). Marine fungi. *Curr Biol*
329 *29*, R191-R195.
- 330 3. Amend, A., Burgaud, G., Cunliffe, M., Edgcomb, V.P., Ettinger, C.L., Gutierrez,
331 M.H., Heitman, J., Hom, E.F.Y., Ianiri, G., Jones, A.C., et al. (2019). Fungi in the
332 Marine Environment: Open Questions and Unsolved Problems. *mBio* *10*.
- 333 4. Nurse, P., and Hayles, J. (2019). Using genetics to understand biology. *Heredity*
334 (Edinb) *123*, 4-13.
- 335 5. Osmani, S.A., and Mirabito, P.M. (2004). The early impact of genetics on our
336 understanding of cell cycle regulation in *Aspergillus nidulans*. *Fungal Genet Biol*
337 *41*, 401-410.
- 338 6. Feyder, S., De Craene, J.O., Bar, S., Bertazzi, D.L., and Friant, S. (2015).
339 Membrane trafficking in the yeast *Saccharomyces cerevisiae* model. *Int J Mol Sci*
340 *16*, 1509-1525.
- 341 7. Mitchison-Field, L.M.Y., Vargas-Muniz, J.M., Stormo, B.M., Vogt, E.J.D., Van
342 Dierdonck, S., Pelletier, J.F., Ehrlich, C., Lew, D.J., Field, C.M., and Gladfelter,
343 A.S. (2019). Unconventional Cell Division Cycles from Marine-Derived Yeasts.
344 *Curr Biol* *29*, 3439-3456 e3435.
- 345 8. Edzuka, T., Yamada, L., Kanamaru, K., Sawada, H., and Goshima, G. (2014).
346 Identification of the augmin complex in the filamentous fungus *Aspergillus*
347 *nidulans*. *PLoS One* *9*, e101471.
- 348 9. Kopecka, M., Gabriel, M., Takeo, K., Yamaguchi, M., Svoboda, A., and Hata, K.
349 (2003). Analysis of microtubules and F-actin structures in hyphae and conidia
350 development of the opportunistic human pathogenic black yeast *Aureobasidium*
351 *pullulans*. *Microbiology (Reading)* *149*, 865-876.
- 352 10. Juanes, M.A., and Piatti, S. (2016). The final cut: cell polarity meets cytokinesis
353 at the bud neck in *S. cerevisiae*. *Cell Mol Life Sci* *73*, 3115-3136.
- 354 11. Wood, E., and Nurse, P. (2015). Sizing up to divide: mitotic cell-size control in
355 fission yeast. *Annu Rev Cell Dev Biol* *31*, 11-29.
- 356 12. Gladfelter, A.S., Hungerbuehler, A.K., and Philippsen, P. (2006). Asynchronous
357 nuclear division cycles in multinucleated cells. *J Cell Biol* *172*, 347-362.
- 358 13. Fischer, R. (1999). Nuclear movement in filamentous fungi. *FEMS Microbiol Rev*
359 *23*, 39-68.
- 360 14. Haraguchi, T., Ding, D.Q., Yamamoto, A., Kaneda, T., Koujin, T., and Hiraoka,
361 Y. (1999). Multiple-color fluorescence imaging of chromosomes and
362 microtubules in living cells. *Cell Struct Funct* *24*, 291-298.
- 363 15. Adams, T.H., Wieser, J.K., and Yu, J.H. (1998). Asexual sporulation in
364 *Aspergillus nidulans*. *Microbiol Mol Biol Rev* *62*, 35-54.

- 365 16. Merson-Davies, L.A., and Odds, F.C. (1989). A morphology index for
366 characterization of cell shape in *Candida albicans*. *J Gen Microbiol* *135*, 3143-
367 3152.
- 368 17. Sudbery, P., Gow, N., and Berman, J. (2004). The distinct morphogenic states of
369 *Candida albicans*. *Trends Microbiol* *12*, 317-324.

370
371

372 **Supplementary video legends**

373

374 **Video 1. Cell division of marine-derived budding yeast**

375 Time-lapse imaging of two budding yeast species (5-min intervals). The budding site is
376 variable (left) or fixed (right) depending on the species.

377

378 **Video 2. Cell division of rod-shaped fungi *Ustilago sp.*, *Leucosporidium intermedium*, 379 and *Sphaerulina rhabdoclinis***

380 Time-lapse imaging of three fungi that have a rod shape and form yeast-like colonies on
381 the plate (5-min interval).

382

383 **Video 3. Cell division of the black yeast *Aureobasidium pullulans***

384 Live imaging of *Aureobasidium pullulans* (NU67) at four different initial cell densities.
385 Images were acquired every 15 min.

386

387 **Video 4. Cell division of the black yeast *Hortaea werneckii***

388 Live imaging of *Hortaea werneckii* (NU28) at three different initial cell densities (lower
389 left, high: upper left, medium: right, low). Images were acquired every 15 min.

390

391 **Video 5. Cell division of an unidentified black yeast species**

392 Live imaging of NU30 (unnamed) at three different initial cell densities (lower left, high:
393 upper left, medium: right, low). Images were acquired every 15 min.

394

395 **Video 6. Nuclear dynamics in the black yeast *Hortaea werneckii* – budding and fission**

396 Live imaging of chromosomes in *Hortaea werneckii* (NU28) during budding- and fission-
397 type mitosis. Images were acquired every 2 min.

398

399 **Video 7. Nuclear dynamics in the black yeast *Hortaea werneckii* – growing tip**

400 Live imaging of chromosomes in *Hortaea werneckii* (NU28) during mitosis of tip-
401 growing cells. Images were acquired every 5 min. Note that flare-like structures are also
402 stained.

403

404

405 **Table 2. List of marine fungi identified in this study (alphabetical order)**

ID	Species	Site	Collection type	*1	*2
NU15	<i>Alternaria chlamyospora</i>	outdoor tank	Bryopsis		n.d.
NU14	<i>Arthopyrenia salicis</i>	rope at pier	Ulva		n.d.
NU29	<i>Arthrimum arundinis</i>	outdoor tank	surface water		n.d.
NU11	<i>Aspergillus protuberus</i>	rope at pier	Undaria		n.d.
NU47	<i>Aspergillus tabacinus</i>	intertidal zone	Lomentaria		n.d.
NU33	<i>Aspergillus versicolor</i>	water at pier tip	surface water		n.d.
NU41	<i>Aspergillus westerdijkiae</i>	intertidal zone	Undaria		n.d.
NU67	<i>Aureobasidium pullulans</i>	water at pier tip	surface water		
NU45	<i>Candida sake</i>	intertidal zone	Codium		
NU56	<i>Cladosporium halotolerans</i>	intertidal zone	Lomentaria		n.d.
NU19	<i>Cladosporium sp. (1)</i>	outdoor tank	surface water		n.d.
NU22	<i>Cladosporium sp. (2)</i>	outdoor tank	surface water		n.d.
NU26	<i>Cladosporium sp. (3)</i>	outdoor tank	surface water		n.d.
NU13	<i>Cladosporium sp. (4)</i>	outdoor tank	Codium		n.d.
NU34	<i>Cladosporium sp. (5)</i>	intertidal zone	Lomentaria		n.d.
NU4	<i>Cladosporium sp. (6)</i>	outdoor tank	sediment		n.d.
NU6	<i>Cystobasidium slooffiae</i>	rope at pier	Undaria		
NU59	<i>Diaporthe sp.</i>	intertidal zone	Spatoglossum		n.d.
NU40	<i>Didymella heteroderae</i>	intertidal zone	Ulva		n.d.
NU64	<i>Didymella sp.</i>	intertidal zone	Codium		n.d.
NU39	<i>Epicoccum laticollum (or E. sorghinum)</i>	intertidal zone	Champia		n.d.
NU49	<i>Filobasidium magnum</i>	intertidal zone	Ulva		
NU24	<i>Filobasidium sp. (likely unreported species)</i>	outdoor tank	surface water		
NU37	<i>Fusarium incarnatum</i>	intertidal zone	Champia		n.d.
NU28	<i>Hortaea werneckii (1)</i>	outdoor tank	surface water		
NU32	<i>Hortaea werneckii (2)</i>	water at pier tip	surface water		
NU2	<i>Kluyveromyces nonfermentans</i>	outdoor tank	sediment		
NU42	<i>Letendreaa sp.(1)</i>	intertidal zone	Undaria		n.d.
NU54	<i>Letendreaa sp.(2)</i>	intertidal zone	Codium		n.d.




NU61	<i>Leucosporidium intermedium</i>	intertidal zone	Undaria		
NU27	<i>Metschnikowia bicuspidata</i>	outdoor tank	surface water		
NU73	<i>Meyerozyma guilliermondii</i>	water at pier tip	surface water		
NU69	<i>Microdochium sp.</i>	water at pier tip	surface water		n.d.
NU65	<i>Neoascochyta paspali</i>	intertidal zone	Laurencia-like		n.d.
NU46	<i>Neopestalotiopsis clavispora</i>	intertidal zone	Lomentaria		n.d.
NU48	<i>Neopestalotiopsis sp.</i>	intertidal zone	Champia		n.d.
NU21	<i>Paraboeremia putaminum</i>	outdoor tank	surface water		n.d.
NU57	<i>Paradendryphiella arenariae</i>	intertidal zone	Champia		n.d.
NU18	<i>Parengyodontium album</i>	outdoor tank	Dasya		n.d.
NU36	<i>Penicillium brasilianum</i>	intertidal zone	Grateloupia		n.d.
NU38	<i>Penicillium brevicompactum</i>	intertidal zone	Champia		n.d.
NU52	<i>Penicillium janczewskii</i>	intertidal zone	Fushitsunagia		n.d.
NU20	<i>Penicillium citrinum</i>	outdoor tank	surface water		n.d.
NU5	<i>Penicillium concentricum</i>	outdoor tank	sediment		n.d.
NU71	<i>Penicillium glandicola</i>	intertidal zone	Colpomenia		n.d.
NU55	<i>Penicillium lenticrescens</i>	intertidal zone	Laurencia-like		n.d.
NU51	<i>Penicillium magnielliptisporum</i>	intertidal zone	Fushitsunagia		n.d.
NU3	<i>Penicillium marinum</i>	outdoor tank	sediment		n.d.
NU53	<i>Penicillium sp.</i> (could be <i>P. sclerotiorum</i> or <i>P. multicolor</i>)	intertidal zone	Colpomenia		n.d.
NU62	<i>Penicillium sp. (or P. alogum)</i>	intertidal zone	Fushitsunagia		n.d.
NU44	<i>Pestalotiopsis portugalica</i>	intertidal zone	Colpomenia		n.d.
NU1	<i>Pestalotiopsis sp</i>	outdoor tank	sediment		n.d.
NU25	<i>Phacidium sp. (WJL-2020c)</i>	outdoor tank	surface water		n.d.
NU43	<i>Phoma moricola</i>	intertidal zone	Fushitsunagia		n.d.
NU35	<i>Pithomyces chartarum or Pseudopithomyces palmicola or Leptosphaerulina chartarum</i>	intertidal zone	Lomentaria		n.d.
NU50	<i>Pyrenochaetopsis</i> (likely <i>P. microspore</i> , <i>P. poae</i> , or <i>P. aff. melioloides</i>)	intertidal zone	Undaria		n.d.
NU68	<i>Rhodotorula babjevae (or R. glutinis)</i>	water at pier tip	surface water		

NU17	<i>Simplicillium lanosoniveum</i>	buoy at pier	Polysiphonia OR Melanothamnus		n.d.
NU58	<i>Sphaerulina rhabdoclinis</i>	intertidal zone	Champia		
NU70	<i>Sphaerulina sp.</i>	intertidal zone	Fushitsunagia		
NU72	<i>Trichoderma atroviride</i>	intertidal zone	Spatoglossum		n.d.
NU23	<i>Umbelopsis isabellina</i>	outdoor tank	surface water		n.d.
NU31	<i>Ustilago sp.</i>	outdoor tank	surface water		
NU63	Unclear	intertidal zone	Colpomenia		n.d.
NU30	Unclear	outdoor tank	surface water		
NU74	Unclear (possibly <i>Didymosphaeriaceae</i>)	water at pier tip	surface water		n.d.





406

407

***1 Comparison with the fungal list of Mitchison-Field et al. (2019)**

	same species identified
	same genus, but not species, identified
	unidentified genus

***2 Division type**

	budding, site fixed
	budding, site variable
	density-dependent
	multiple fissions
	rod shaped, budding

408

Figure 1

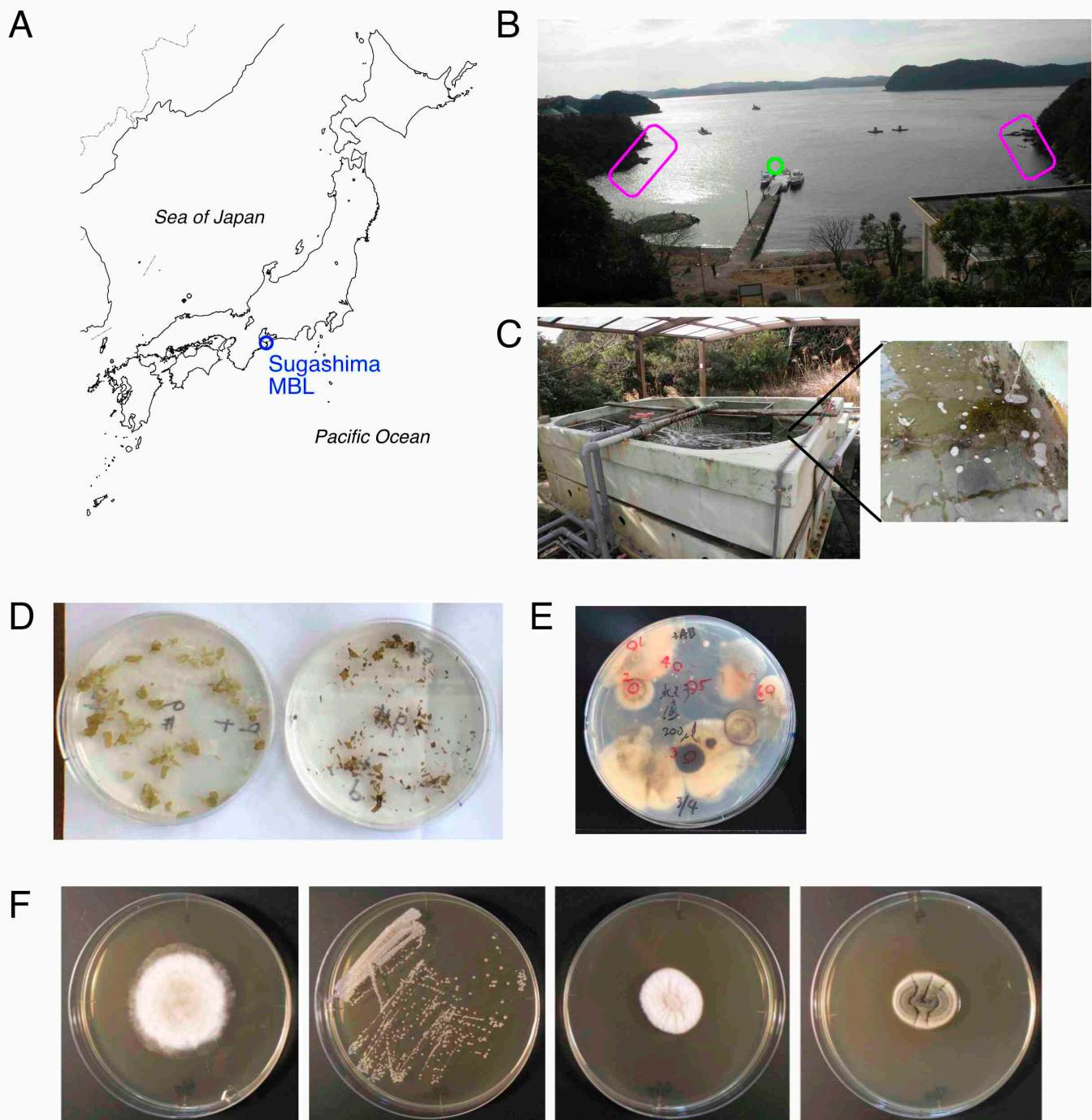


Figure 1. Collection of marine fungi from surface ocean water, sediment, and seaweeds

(A) Location of Sugashima Marine Biological Laboratory (NU-MBL). (B) Surface ocean water was obtained at the pier (green), whereas seaweeds were collected at the intertidal zone (magenta). (C) Outdoor tank at NU-MBL which has a continuous flow of unfiltered sea water. The sediment and surface water were the sources of marine fungi. (D) Severed seaweeds on the fungal medium plate. Several fungal colonies grew after several days. (E) Examples of fungal colonies on the plate (sediment sample). Each colony was marked and subjected to genotyping PCR and transfer to a fresh plate. (F) Examples of fungal colonies on YPD plates (NU1 – 4). Filamentous fungi were inoculated onto the centre of the plate, whereas yeasts were streaked. The diameter of the plates in this figure is 9 cm.

Figure 2

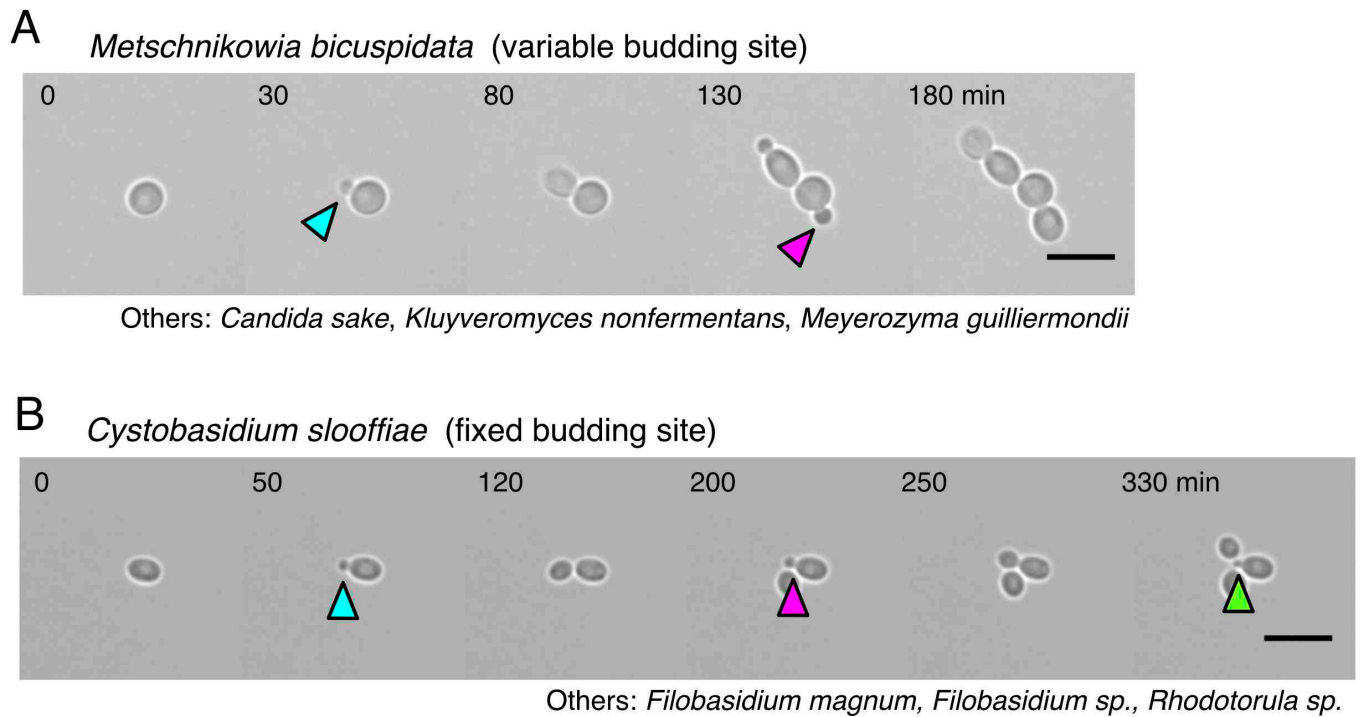


Figure 2. Budding yeast has either a fixed or variable budding site

(A) *S. cerevisiae*-type budding yeast, where a bud emerges at seemingly random sites on the round mother cell. (B) The budding site is fixed at one site of the mother cell. Blue arrows, initially emerged bud; magenta arrow, second bud; green arrow, third bud. Scale bars, 10 μ m.

Figure 3

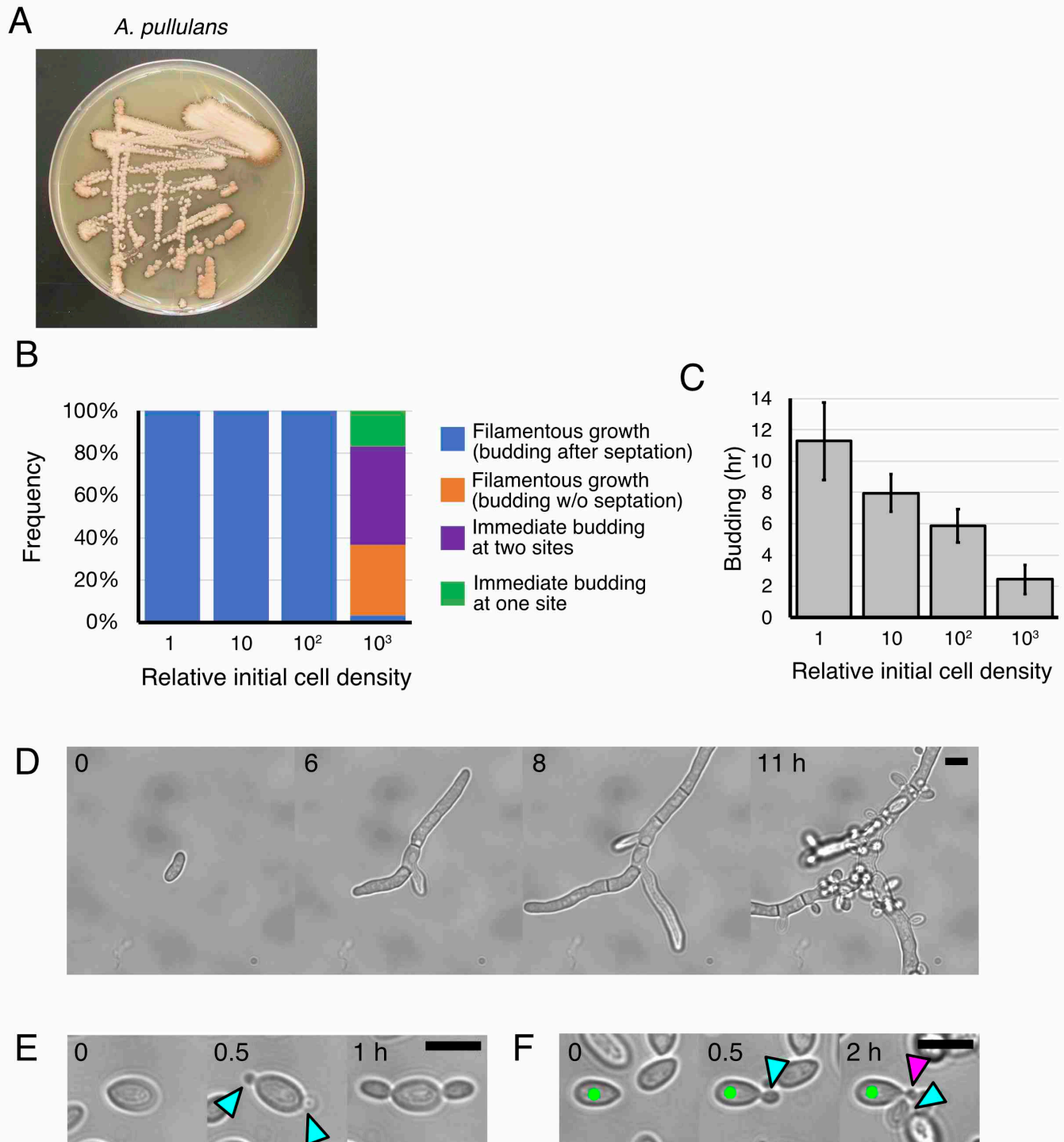


Figure 3. Division pattern variation in the black yeast *Aureobasidium pullulans*

(A) *A. pullulans* colonies. The peripheries of the colonies turned brown after prolonged storage at 4 °C (fresh colonies are uncoloured). (B) Four distinct bud formation patterns dependent on the initial cell density. Saturated cultures were diluted at four different concentrations, and the growth and budding style was assessed ($n = 7, 18, 25, 30$ [left to right]). (C) Timing of bud emergence after a cell started to grow in a filamentous manner (\pm SD) ($n = 7, 18, 25, 11$ [left to right]). (D) Filamentous growth with occasional septation and branching, followed by budding from various sites on the filament. This mode of growth/budding was dominant when the initial cell density was low. (E, F) Immediate budding without apparent cell growth or septation. Two buds simultaneously emerged at two opposite sites in (E), whereas two buds sequentially emerged at one site of the mother cell in (F). Blue arrows, initially emerged buds; magenta arrow, second bud; green, mother cell. Scale bars, 10 μ m.

Figure 4

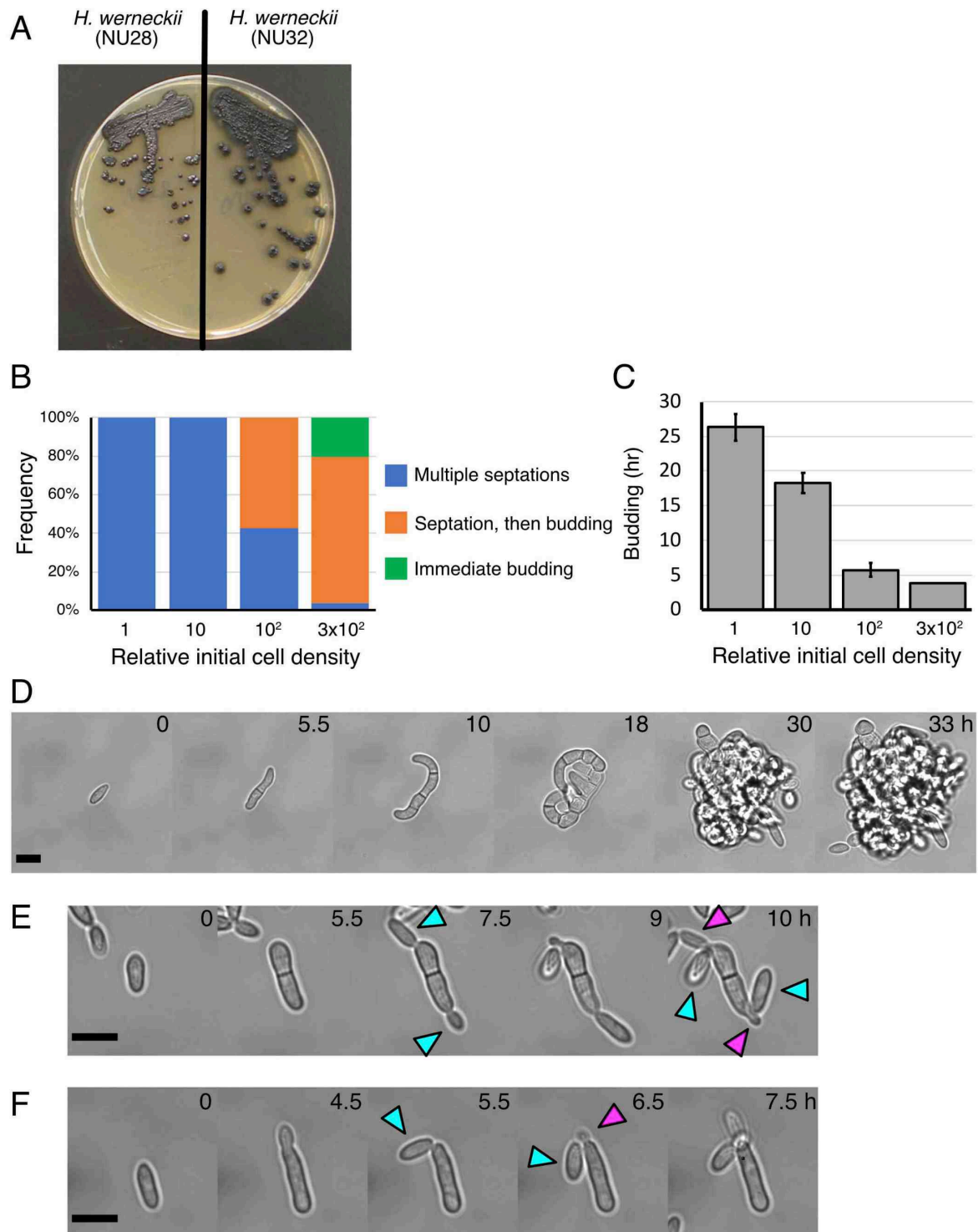


Figure 4. Division pattern variation in the black yeast *Hortaea werneckii*

(A) Colonies of two *H. werneckii* strains, which had different growth rates. (B) Three distinct bud formation patterns dependent on the initial cell density. Saturated cultures were diluted at four different concentrations, and the growth and budding style was assessed ($n = 19, 11, 28, 54$ [left to right]). (C) Timing of bud formation after the first septation (\pm SD) ($n = 19, 11, 12, 2$ [left to right]). Because the sample size was low, SD was not provided in the condition with the highest density. (D) Filamentous growth with septation and branching, followed by budding from various sites on the curved filament (a released bud is seen at lower-left corner at 43 h). This mode of growth/budding was dominant when the initial cell density was low. (E) Elongation, septation, followed by budding. Multiple buds sequentially emerged from a “mother” cell that had undergone septation. This mode of septation/budding was dominant when the initial cell density was high. (F) Immediate budding without septation. Multiple buds sequentially emerged from a “mother” cell. Blue and magenta arrows indicate the first and second buds, respectively. Scale bars, 10 μ m.

Figure 5

A *black yeast* "NU30"

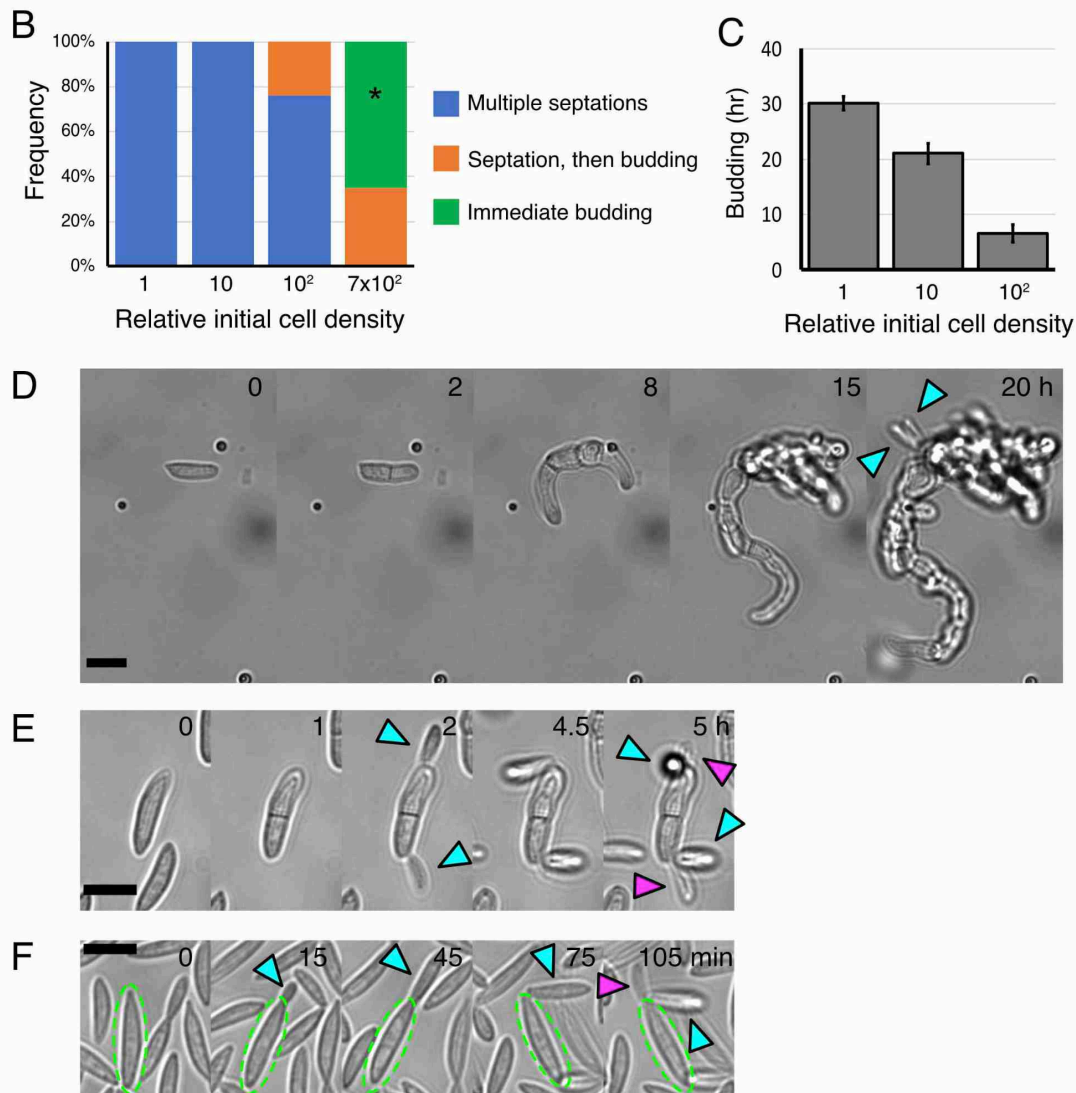


Figure 5. Division pattern variation in an unidentified black yeast species "NU30"

(A) Colonies of NU30. Each colony turned dark brown after prolonged storage at 4 °C (fresh colonies were uncoloured). (B) Three distinct bud formation patterns dependent on the initial cell density. Saturated cultures were diluted at four different concentrations, and the growth and budding style was assessed (n = 12, 12, 25, 37 [left to right]). Asterisk: the frequency of immediately budding cells was underestimated, as many cells did not stick to the glass and were hard to count, whereas all the cells that underwent septations were immobile and countable. (C) Timing of bud formation after the first septation (\pm SD) for the cells that formed multiple septations (n = 12, 12, 19 [left to right]). (D) Filamentous growth with septation and branching, followed by budding from various sites on the curved filament (20 h). This mode of growth/budding was dominant when the initial cell density was low. (E) Single septation, followed by budding. Multiple buds sequentially emerged from a "mother" cell that had undergone septation. (F) Immediate budding without septation. Multiple buds sequentially emerged from the "mother" cell (green). This mode of budding was dominant when the initial cell density was high. Blue and magenta arrows indicate the first and second buds, respectively. Scale bars, 10 μ m.

Figure 6

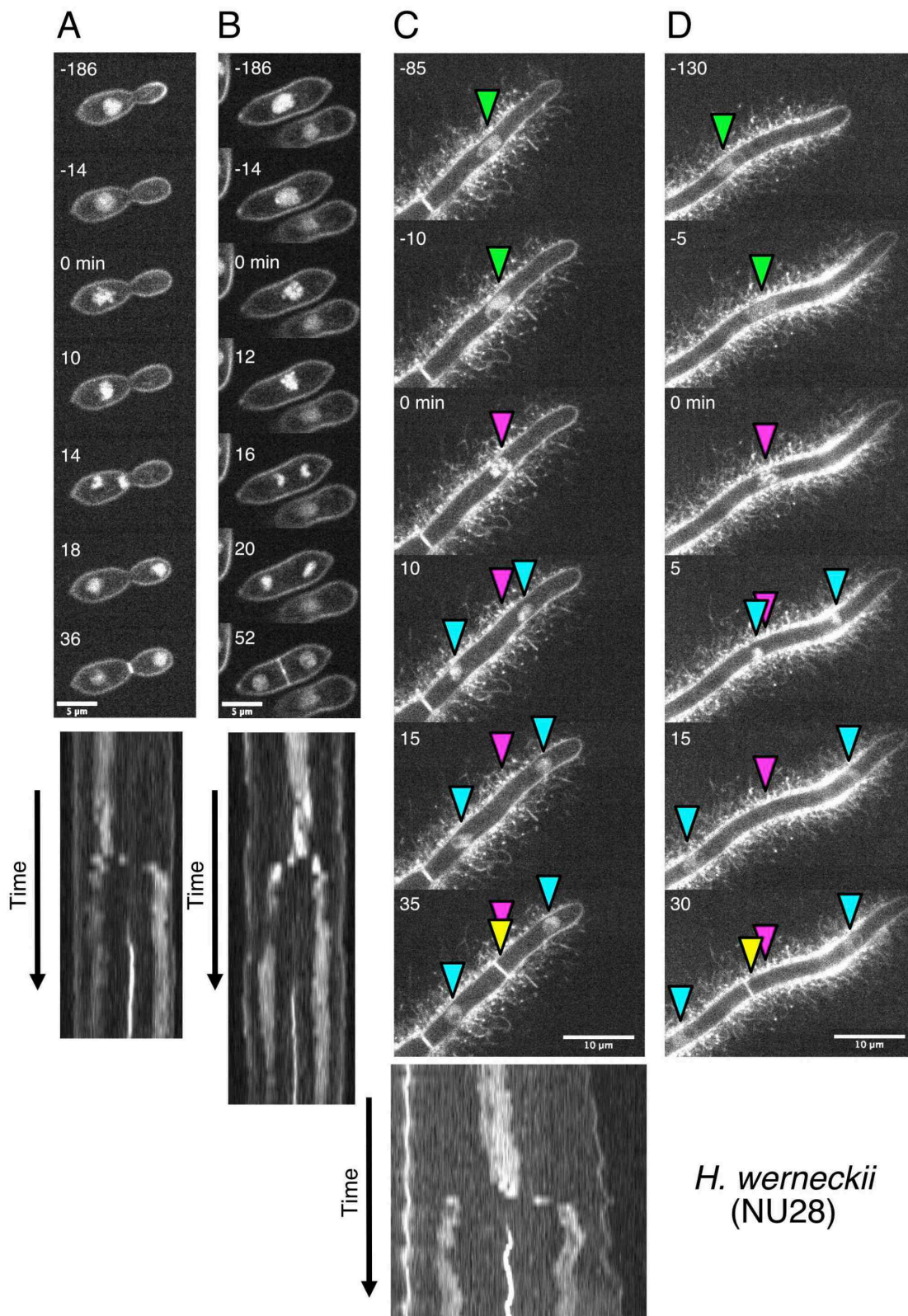


Figure 6. Nuclear dynamics in *H. werneckii*

(A) Nuclear dynamics during budding-type cell division. The corresponding kymograph is shown at the bottom. Time 0 indicates mitotic entry. (B) Nuclear dynamics during fission-type cell division. The corresponding kymograph is shown at the bottom. Time 0 indicates mitotic entry. (C, D) Nuclear dynamics in tip-growing cells. Green arrowheads, interphase nuclei; magenta, position of condensed chromosomes at the mitotic entry; blue, sister chromatids/nuclei; yellow, septum. Septum was formed at the site of mitotic chromosomes in (C), whereas it was deviated in (D). Segregation of sister chromatids is asymmetric relative to the metaphase chromosome. The corresponding kymograph is shown at the bottom.